RAFT/MADIX emulsion copolymerization of vinyl acetate and N-vinylcaprolactam: towards waterborne physically crosslinked thermoresponsive particles

Laura Etchenausia, Abdel Khoukh, Elise Deniau-Lejeune, Maud Save

RAFT/MADIX emulsion copolymerization of vinyl acetate and *N*-vinylcaprolactam: towards waterborne physically crosslinked thermoresponsive particles

Laura Etchenausia, Abdel Khoukh, Elise Deniau Lejeune, Maud Save*

CNRS, University Pau & Pays Adour, Institut des Sciences Analytiques et de Physico-Chimie pour l'Environnement et les Matériaux, IPREM, UMR5254, Equipe de Physique et Chimie des Polymères, 64000, PAU, France

E-mail: maud.save@univ-pau.fr

ABSTRACT

Well-defined poly(*N*-vinylcaprolactam-*co*-vinyl acetate) thermoresponsive particles physically crosslinked by means of hydrophobic interactions were synthesized by polymerization-induced self-assembly. It was highlighted that a xanthate-terminated poly(ethylene glycol) (PEG-X) efficiently acted as both stabilizer and macromolecular chain transfer agent for the RAFT/MADIX batch emulsion copolymerization of *N*-vinylcaprolactam (VCL) and vinyl acetate (VAc), enabling the direct synthesis in aqueous dispersed media of PEG-*b*-P(VAc-*co*-VCL) block copolymers. It was emphasized that a fraction of 47 mol-% of hydrophobic VAc in the second block of the copolymer was suitable to maintain the integrity of the self-assembled PEG-*b*-P(VAc-*co*-VCL) block copolymer particles at low temperature while exhibiting a temperature-induced phase transition. The well-defined physically crosslinked particles interestingly behaved as thermoresponsive colloids analogue to chemically crosslinked microgels. The PEG-*b*-P($VAc_{0.47}$-*co*-$VCL_{0.53}$) particles were able to undergo a reversible swollen-to-collapse transition with increasing temperature in the absence of hysteresis. The PEG-*b*-P($VAc_{0.17}$-*co*-$VCL_{0.83}$) block copolymer with a lower fraction of VAc in the copolymer (17 mol-%) behaved oppositely as very small objects were present in the aqueous phase at low temperature (T < 20 °C) and self-assembled into large aggregates by rising the temperature. Finally, the statistical copolymers based on VAc and VCL were successfully hydrolyzed into promising thermoresponsive biocompatible statistical copolymers based on vinyl alcohol and *N*-vinylcaprolactam co-monomer units.

INTRODUCTION

Waterborne latex produced by the environmentally friendly and industrially relevant emulsion polymerization process is a class of materials with myriad of applications in paints, adhesives, rubbers, coatings, concrete additive and nonwoven fabric, but also in cosmetics, biomaterials and other high-tech areas.[1] Stimuli-responsive polymers are a class of advanced polymers exhibiting properties tuned by an external stimulus such as temperature, light, pH, organic or gaseous molecules.[2-5] These polymers have received considerable attention within the last decade, due to their wide range of applications for smart materials like responsive optical devices[6, 7], membrane technology,[8, 9] or for biomaterials like drug delivery systems, biosensors or cell culture substrates.[10-14] It is thus relevant to produce stimuli-responsive polymers of controlled macromolecular features as waterborne latex by emulsion polymerization process.

In the early 2000s, different research groups have made tremendous efforts to transpose the control of radical polymerization from homogeneous systems (bulk, solution) to heterogeneous systems and especially to the industrially relevant emulsion polymerization process performed in aqueous dispersed media.[15-17] Indeed, the emulsion polymerization process presents many advantages compared to polymerizations performed in bulk or in organic solution. In fact, the use of water as continuous phase facilitates heat transfer of the exothermic polymerization, decreases the viscosity of the final product which facilitates polymer recovery from the reactor at the end of the polymerization, and is more environmentally safe by limiting the amount of volatile organic compounds. As reported in several reviews,[15-17] most of the investigations focused on controlling the polymerization in aqueous dispersed media of (meth)acrylic or styrenic monomers, while very few studies concerned less activated monomers (LAM) such as vinyl acetate (VAc)[18-25] or vinyl chloride (VC).[26] Note that, despite the interesting features of the biocompatible thermoresponsive poly(*N*-vinylcaprolactam) (PVCL),[27] controlled radical polymerization of VCL by polymerization in aqueous dispersed media has never been investigated up to now. Among the different strategies investigated to implement controlled radical polymerization in aqueous dispersed media, the *in-situ* formation of amphiphilic diblock copolymers simultaneously to the particle growing via emulsion polymerization process, in a concept known as *"polymerization-induced self-assembly"* (PISA), has emerged as one of the most efficient method.[28] PISA simultaneously addresses several challenges. The use of the reactive hydrophilic polymer producing the initial block copolymer micelles overcame the issue of diffusion of the hydrophobic control agent to the loci of

polymerization, hence offering the opportunity to implement controlled radical polymerization in a batch *ab initio* emulsion polymerization process.[29, 30] Moreover, it is a straightforward method to synthesize stable hairy particles at high solids content by surfactant-free emulsion polymerization. Finally, it is an alternative route to produce self-assembled block copolymer nano-objects of various morphologies dispersed in water by a one-step method.[28, 31, 32] The PISA concept applied with thermoresponsive growing block was recently termed polymerization-induced thermal self-assembly (PITSA).[33] The pioneering works of using a reactive macromolecular stabilizer for the design of thermoresponsive particles dealt with chemically crosslinked particles.[34-36] Delaittre *et al.* reported the benefits provided by PISA to straightforwardly synthesize physically crosslinked poly(*N,N*-diethylacrylamide)-based thermoresponsive spherical particles via a reactive poly(acrylic acid) macroalkoxyamine.[37] Physically crosslinked microgels are a class of interesting supramolecular particles linked via reversible non-covalent interactions to create dynamic particles.[38]

Among the stimuli-responsive polymers, thermoresponsive polymers are a class of relevant polymers which undergo a conformation phase transition in response to a change of temperature.[12] The most extensively studied thermoresponsive polymer is the poly(*N*-isopropylacrylamide) (PNIPAAm) with a LCST of 32°C close to the physiological temperature. Over the last ten years, poly(oligo(ethylene glycol) (meth)acrylates) (P(OEG)(M)A)[39-41] or poly(*N*-vinylcaprolactam) (PVCL),[27, 42] which also present a LCST near to physiological temperature, have emerged as biocompatible thermoresponsive polymers of interest. Poly(*N*-vinylcaprolactam) is a 7-membered ring type polymer which is biocompatible, water-soluble, non-ionic and exhibits a LCST in water ranging between 30 and 40°C.[27, 42-44 42, 45-47] As for other thermoresponsive polymers, the temperature in which the change of PVCL chain solvation state occurs can be tuned by introducing co-monomers in the polymer chains.[48-51] Among the different co-monomers that can be used to tune the phase transition temperature of PVCL chains in water, vinyl acetate (VAc) is an attractive co-monomer to simultaneously promote non-covalent hydrophobic interactions. Moreover, poly(vinyl acetate) (PVAc) is used in a vast number of applications, the most common being binder for adhesive formulation, for the paper industry and for latex paints.[52, 53] Particularly, PVAc is approved by Food and Drug Administration (FDA) and it is a precursor of poly(vinyl alcohol) (PVA) which is a biocompatible and biodegradable hydrophilic polymer that is used in many technical (textile, papermaking) or food applications.[53] PVA is for instance used as efficient

thickener, protective colloids, component of water-soluble film useful for packaging.[53] Nowadays, the raw materials for vinyl acetate monomer are produced from fossil resources. In the context of sustainable development, it can be mentioned that bioethanol produced from renewable resource could substitute the feedstock for these raw materials. Therefore, if the "vinyl acetate circle" can be closed by the important steps of hydrolysis and complete biodegradation of vinyl ester-based polymers to carbon dioxide, the whole production of PVAc could be switched to a renewable, sustainable and CO_2-neutral production process based on bioethanol.[53]

Herein, we present the first example of emulsion copolymerization of VCL and VAc mediated by a xanthate-functionalized poly(ethylene glycol) (PEG-X) as the reactive macromolecular chain transfer agent to follow the PISA mechanism. Our previous work demonstrated that xanthate–mediated RAFT/MADIX copolymerization of VAc/VCL was well-controlled in bulk with a close reactivity of both monomers (r_{VAc} = 0.33 and r_{VCL} = 0.29).[54] These P(VAc-*co*-PVCL) amphiphilic copolymers of homogeneous distribution exhibited tunable phase transition temperature (PTT) and self-assembly behavior depending on the fraction of hydrophobic VAc. Indeed, static and dynamic light scattering measurements highlighted that P(VAc-*co*-VCL) copolymer with F_{VAc} = 0.53 had the capability to self-assemble in water into trimer aggregates at a temperature below the cloud point temperature, by means of hydrophobic interactions. The dual objective of the present work is to synthesize the amphiphilic thermoresponsive PEG-*b*-P(VAc-*co*-VCL) block copolymers of controlled molar mass directly in aqueous dispersed media while providing the opportunity to prepare thermoresponsive particles physically crosslinked by hydrophobic interactions. Insight into the control of RAFT/MADIX emulsion copolymerization of VAc and VCL as well as the features of the synthesized thermoresponsive colloidal particles, in relationship with the initial VAc monomer feed ratio is provided. Moreover, as poly(vinyl alcohol) (PVA) is a biocompatible polymer of interest for a wide field of applications, thermoresponsive PVA-based statistical copolymers are prepared by hydrolysis of the PEG-*b*-P(VAc-*co*-VCL) precursor copolymers.

EXPERIMENTAL PART

Materials

Vinyl acetate (VAc, Sigma Aldrich, 99 %+) was mixed with inhibitor removers (Sigma Aldrich, 0.1 g of inhibitor remover for 50 mL of VAc) for 30 min prior to be filtered and used for polymerization. *N*-vinylcaprolactam (VCL, Sigma Aldrich, 98 %), Poly(ethylene glycol) methyl ether (PEG-OH, M_n = 2 000 g.mol^{-1}, Sigma Aldrich), 2-bromopropionyl bromide (Sigma Aldrich, 97 %), anhydrous dichloromethane (Sigma Aldrich, 99,8 %), triethylamine (Sigma Aldrich, 99 %), potassium ethyl xanthogenate (Sigma Aldrich, 96 %), tris(hydroxymethyl)aminomethane hydrochloride buffer (TRIZMA, Sigma Aldrich, 99 %), potassium hydroxide (Sigma Aldrich, 90 %), methanol (Sigma Aldrich, 99,8 %) and 2,2'-Azobis[2-(2-imidazolin-2-yl)propane] dihydrochloride (ADIBA or VA-044, Wako, 99 %) were used as received. For the emulsion copolymerizations double deionized water was used as continuous medium.

Preparation of xanthate-terminated PEG (PEG-X) macro-chain transfer agent (macro-CTA).

The xanthate-terminated PEG macro-CTA was synthesized in a two steps procedure from commercially available PEG-OH, according to an already described procedure (see **Scheme 1** in Supporting Information).[25, 55] In the first step the hydroxyl end-group of PEG-OH was esterified with 2-bromopropionyl bromide, using triethylamine (TEA) as a base. The second step involved the nucleophilic substitution of potassium ethyl xanthogenate with PEG-Br leading to the xanthate-terminated PEG macro-CTA named as PEG-X throughout this work. The proton NMR analysis of PEG-OH, PEG-Br and PEG-X (**Figure S1**) confirms the successful functionalization of the PEG chain-end. The perfect overlay of the UV-visible (λ = 355 nm) and RI traces of the SEC chromatograms of PEG-X also corroborates a high level of chain-end functionalization with the presence of the dithiocarbonate chain-end over the entire molar mass distribution (**Figure S2**).

General procedure for the RAFT/MADIX emulsion copolymerization of VAc and VCL mediated by a xanthate-terminated PEG macro-CTA.

The reactions were carried out at 10 wt-% of initial solids content, with different initial molar fractions of VAc ($f_{VAc,0}$ = 0.2, expt 1 in **Table 1** and $f_{VAc,0}$ = 0.5, expt 2 in **Table 1**). For both experiments, the $[Monomer]_0/[PEG\text{-}X]_0$ and $[PEG\text{-}X]_0/[ADIBA]_0$ ratios were respectively set at 430 and 3.2. As example of experiment 2 in **Table 1**, 1,3,5-trioxane (0.40 g, 4.4 × 10^{-3} mol), TRIZMA buffer (0.15 g, 9.5 × 10^{-4} mol), PEG-X (0.30 g, 1.0 × 10^{-4} mol), *N*-vinylcaprolactam (3.10

g, 2.2×10^{-2} mol), vinyl acetate (1.90 g, 2.2×10^{-2} mol) and deionized water (48.00 g) were introduced in a 100 mL round-bottom flask and the mixture was purged with nitrogen for 30 min in an ice-bath. A sample was withdrawn under nitrogen at time $t = 0$. The round-bottom flask was placed into an oil-bath previously heated to 65°C. The cationic initiator was added under nitrogen flow at 65°C (10.40 mg of ADIBA dissolved in 2 g of deionized water, 3.2×10^{-5} mol of ADIBA). The polymerization reaction was then allowed to continue with 300 rpm stirring for 5 h 30 min at 65°C. At the end of the reaction, a sample was withdrawn and kept at 65°C for DLS analysis. The reaction mixture was subsequently cooled to 25°C and oxygen was introduced in the reaction mixture. The same protocol was followed for the free radical emulsion copolymerization of VAc and VCL using PEG-OH as stabilizer (expt 3 in **Table 1**). The final copolymers were dialyzed against a 3.5 kDa cut-off membrane and freeze-dried prior SEC and turbidimetry analyses.

Alkaline hydrolysis of the PEG-*b*-P(VAc-*co*-VCL) copolymers

In a typical experiment, the dialyzed (M_w cut-off: 3500 Da) and freeze-dried PEG-*b*-P($VAc_{0.17}$-*co*-$VCL_{0.83}$), (expt 1 in **Table 1**, 0.10 g, 6.2×10^{-6} mol of copolymer) was introduced in a 10 mL round-bottom flask and dissolved in 2.9 g of methanol. A solution of 38.1 mg of KOH (6.8×10^{-4} mol, [KOH] = 1.4×10^{-1} mol.L^{-1}) dissolved in 1.0 g of methanol was then added to the flask. The mixture was stirred at room temperature for 18 h. Subsequently, the solution was dialyzed against distilled water through a Spectra/Pore membrane (6-8 kDa cut-off membrane) for 7 days and the PEG-*b*-P(VA-*co*-VCL) copolymer was recovered by freeze-drying. The same procedure was followed for the alkaline hydrolysis of PEG-*b*-P($VAc_{0.47}$-*co*-$VCL_{0.53}$) copolymer (expt 2 in **Table 1**).

Characterization method

Nuclear Magnetic Resonance (NMR) spectroscopy. NMR spectra were recorded using a Brüker 400 MHz spectrometer, at 25°C, except for the characterization of PEG-*b*-P(VA-*co*-VCL) copolymers which was performed at 80°C. ^{1}H measurements were performed at frequencies of 400 MHz and ^{13}C measurements at 100 MHz. ^{13}C quantitative spectra are taken without Nuclear Overhauser Effect and with a long relaxation delay (10 s). This decoupling mode is referred to as inverse-gated (zgig as 1D Bruker pulse sequence).

The final overall molar monomer conversion (X_m) was calculated from nuclear magnetic resonance spectra in acetone-d_6 using 1,3,5-trioxane as internal standard (**Equation 1** and **Figure S3a**).

$$X_{\mathrm{m}} = 1 - \frac{\left(I_{(1\mathrm{H_{VAc}} + 1\mathrm{H_{VCL}})} / I_{1\mathrm{H_{triox.}}} \right)_t}{\left(I_{(1\mathrm{H_{VAc}} + 1\mathrm{H_{VCL}})} / I_{1\mathrm{H_{triox.}}} \right)_0}$$ Equation 1

$I_{1\mathrm{H,triox}}$ corresponds to the integral of one proton of 1,3,5-trioxane (5.1 ppm, 6 H, *i* protons in **Figure S3a**) used as internal standard and $I_{(1\mathrm{H,VAc} + 1\mathrm{H,VCL})}$ corresponds to the integral of the vinylic protons of both VCL monomer and VAc monomer at 7.1-7.4 ppm ($I_{7.1\text{-}7.4\ \mathrm{ppm}} = I_{1\mathrm{H,VAc}} + I_{1\mathrm{H,VCL}}$, protons *3+c* in **Figure S3a**).

The compositions of the P(VAc-*co*-VCL) blocks (F_{VAc} and F_{VCL}) were calculated on the basis of the integrals of the protons of each polymer unit of ^{1}H NMR spectra (**Equation 2** and **Figure S3b**) and on the basis of the integrals of the well-resolved carbonyl signals at 170 – 180 ppm of each polymer unit of the P(VAc-*co*-VCL) copolymer (**Equation 3** and **Figure S4**).

$$F_{\mathrm{VAc}} = \frac{I_{\mathrm{IV}/3}}{I_{III,C}}$$ Equation 2

$$F_{\mathrm{VAc}} = \frac{I_{\mathrm{C=O,PVAc}}}{I_{\mathrm{C=O,PVAc}} + I_{\mathrm{C=O,PVCL}}}$$ Equation 3

The copolymers synthesized by emulsion polymerization were characterized by DOSY NMR spectroscopy in DMSO-d_6. The DOSY NMR experiments were performed using the bipolar longitudinal eddy current delay pulse sequence (BPLED). The spoil gradients were also applied at the diffusion period and the eddy current delay. Typically, a value of 2 ms was used for the gradient duration (δ), 150 ms for the diffusion time (Δ), and the gradient strength (g) was varied from 1.67 G.cm^{-1} to 31.88 G.cm^{-1} in 32 steps. Each parameter was chosen to obtain 95 % signal attenuation for the slowest diffusion species at the last step experiment. The pulse repetition delay (including acquisition time) between each scan was larger than 2s. Data acquisition and analysis were performed using the Bruker Topspin software (version 2.1). DOSY spectra were generated by using the program GIFA software,[56] the DOSY Module of NMR Notebook from NMRTEC, using inverse Laplace Transform driven by maximum entropy to create 2-D spectra with NMR chemical shifts along one dimension and the calculated diffusion coefficients along the other. The diffusion coefficients were extracted from T1/T2 analysis module of Topspin 2.1.

Size Exclusion Chromatography (SEC). The SEC system operates in THF, at 30°C (flow rate: 1mL.min^{-1}). The SEC apparatus is equipped with a Viscotek VE 5200 automatic injector, a pre-column and two columns (Styragels HR 5E and 4E (7.8 × 300 mm)) working in series, a Wyatt Heleos II Multi Angle Laser Light Scattering detector (MALLS, 18 angles, λ_0 = 664.4 nm), a viscosimeter detector (Wyatt Viscostar II), a refractive index (RI) detector Viscotek VE 3580 and

a Viscotek VE 3210 UV-visible detector. Toluene was used as flow marker. All (co)polymer samples were prepared at 3 $g.L^{-1}$ concentrations. The number-average molar mass (M_n) and molar mass distribution ($Đ$) were obtained from MALLS data using the M_i value of each slice of the chromatogram (Debye plot).

The experimental M_n are compared to the theoretical number-average molar masses of the copolymers calculated from **Equation 4**.

$$Mn_{theo.} = M_{\mathrm{PEG-X}} + X_m \frac{[\mathrm{M}]_0 \times (f_{\mathrm{VAc},0} \times M_{\mathrm{VAc}} + f_{\mathrm{VCL},0} \times M_{\mathrm{VCL}})}{[[\mathrm{PEG-X}]_0 + [\mathrm{Initiator}]_0\ (1-e^{-k_d \times t})]}$$ Equation 4

Where $M_{\mathrm{PEG\text{-}X}}$ corresponds to the molar mass of the PEG-X macromolecular chain-transfer agent ($M_{n,\ \mathrm{PEG\text{-}X,\ MALLS}}$ = 2 240 $g.mol^{-1}$), X_m is the final overall molar conversion calculated from NMR spectra (see Equation 1), k_d is the initiator dissociation constant ($k_{d,\ \mathrm{ADIBA,\ water,\ 70°C}}$[57] = 6.7×10^{-4} s^{-1}), t is the polymerization time, $[\mathrm{Xanthate}]_0$, $[\mathrm{Initiator}]_0$ and $[\mathrm{M}]_0$ are the initial concentrations of respectively the chain-transfer agent, the initiator and monomer ($[\mathrm{M}]_0 = [\mathrm{VAc}]_0 + [\mathrm{VCL}]_0$). $f_{\mathrm{VAc},0}$ and $f_{\mathrm{VCL},0}$ are the initial monomer feed ratios. M_{VAc} and M_{VCL} are the molar masses of each monomer (M_{VCL} = 139 $g.mol^{-1}$ and M_{VAc} = 86 $g.mol^{-1}$).

The refractive index increments (d*n*/d*c*) in THF of the PEG-*b*-P(VAc-*co*-VCL) copolymers were measured: $(dn/dc)_{\mathrm{PEG\text{-}b\text{-}P(VAc0.17\text{-}co\text{-}VCL0.83)}}$ = 0.099 $mL.g^{-1}$ and $(dn/dc)_{\mathrm{PEG\text{-}b\text{-}P(VAc0.47\text{-}co\text{-}VCL0.53)}}$ = 0.088 $mL.g^{-1}$.

Turbidimetry analysis. Prior analysis samples were dialyzed against distilled water through a Spectra/Pore membrane (M_w cut-off: 3500 Da) for 48 h and recovered by freeze-drying. Turbidimetry measurements of the (co)polymers solutions (0.3 wt-% in water) were performed with a Shimadzu UV-2450PC spectrophotometer, from 13°C to 33°C (heating rate: 0.5°C/min). Transmittance at 500 nm was plotted versus the temperature. The minimum of the first-order derivative fit of transmittance versus temperature was considered as the phase transition temperature (PTT).

Dynamic Light Scattering (DLS). The hydrodynamic diameters (D_h) of the latex particles synthesized by emulsion copolymerization of VAc and VCL mediated by xanthate-terminated PEG macromolecular chain-transfer agent were measured at 55°C directly after withdrawing the latex at the end of the polymerization, without cooling step. Before analysis, samples were diluted by a factor 100 in warm distilled water and were characterized with a Vasco DL135 Cordouan Technologies equipment at λ_{laser} = 657 nm. The evolution of the final average hydrodynamic

diameters of aqueous solutions of PEG-*b*-P(VAc-*co*-VCL) copolymers before and after hydrolysis were measured as a function of the temperature, by dynamic light scattering (DLS), using a Zetasizer Nano ZS instrument (Malvern Instruments). A He-Ne 4.0mW power laser was used, operating at a wavelength of 633 nm. For evaluation of the data, the DTS (Nano) program was used. The hydrodynamic diameters were calculated from the diffusion coefficient using the Stokes-Einstein equation $D_h = \frac{k_B T}{3\pi\eta D}$ where T is absolute temperature, η the viscosity of the solvent, k_B the Boltzmann constant and D the diffusion coefficient. For the analysis of PEG-*b*-P(VAc-*co*-VCL), measurements were carried out at a solids content of 0.005 wt-% from 10°C to 55 °C and from 55 °C to 10 °C. The measurements were performed every to 2°C with 10 minutes of equilibrium time at each temperature. The analysis of P(VAc-*co*-VA-*co*-VCL) copolymers dispersed in deionized water were carried out at a concentration of 5 $g.L^{-1}$ from 10°C to 48°C, every 2°C.

Fourier transform Infra-red (FTIR) spectroscopy. Spectra of the dialyzed and freeze-dried PEG-*b*-P(VAc-*co*-VCL) copolymers before and after hydrolysis were recorded on a FTIR NICOLET Magna-IR560, at 25°C. Attenuated total reflectance (ATR) mode was used.

RESULTS AND DISCUSSION

In this work, the xanthate-functionalized poly(ethylene glycol) (PEG-X) is involved as macromolecular chain transfer agent (macro-CTA) in the RAFT/MADIX emulsion copolymerization of VAc and VCL carried out at 65°C, using ADIBA as water-soluble initiator (**Table 1**). On the basis of the results obtained in our previous study concerning the bulk copolymerization of VAc and VCL, the thermoresponsive P(VAc-*co*-VCL) statistical copolymers are insoluble in water at 65°C.[54] Moreover, both monomers are water insoluble at a concentration of 10 wt-% based on water, hence forming monomer droplets at the initial state. It is thus expected that the mechanism will follow an emulsion polymerization process.

Table 1. Experimental conditions for the emulsion copolymerization of VAc and VCL performed at 65°C with 10 wt-% of initial solids content in water.

Expt	$f_{VAc,0}$[a]	$[ADIBA]_0$ *mol.L^{-1}$_{H2O}$*	Stabilizer	$[Stabilizer]_0$ *g.L^{-1}$_{H2O}$*	Stabilizer *wt-% based on monomers*	$\frac{[PEG\text{-}X]_0}{[ADIBA]_0}$	$\frac{[VAc]_0+[VCL]_0}{[PEG\text{-}X]_0}$
1	0.2	5.4×10^{-4}	PEG-X	4.9	5.4	3.2	430
2	0.5	5.9×10^{-4}	PEG-X	5.4	6.0	3.2	430
3	0.5	5.9×10^{-4}	PEG-OH	5.4	6.0	-	-

[a] $f_{VAc,0}$ is the VAc molar fraction in the initial monomer feed.

It should be mentioned that stable latex particles were formed during the course of polymerization in the absence of coagulum or phase separation for both syntheses carried out at different initial monomer feed ratios (see **Table 1** and **Table 2**, expt 1 and 2). This suggests that the PEG-X efficiently acts as steric stabilizer during the emulsion copolymerization of VAc and VCL. Note that 80-85 % of monomer conversion is reached by emulsion copolymerization (**Table 2**) while the monomer conversion was limited to 50-60 % in bulk for a similar 6 h of polymerization (see **Table 2** and reference [54]).

Table 2. Results of emulsion copolymerization of VAc and VCL mediated by PEG-X macromolecular chain transfer agent.[a]

Expt	F_{VAc}[b]	F_{VAc}[c]	X_m[d] *%*	$M_{n,theo}$[e] *g.mol^{-1}*	$M_{n,SEC}$[f] *g.mol^{-1}*	$Đ$[f]	$D_{h,\ 55°C}$[g] *nm*	*Copolymer*
1	0.17	0.17	80	32 520	16 700	1.6	150	PEG-*b*-P($VAc_{0.17}$-*co*-$VCL_{0.83}$)
2	0.47	0.52	85	31 490	19 790	2.0	95	PEG-*b*-P($VAc_{0.47}$-*co*-$VCL_{0.53}$)

[a] 10 wt-% of initial solids content and T = 65°C; [b] Molar fraction of VAc in the P(VAc-*co*-VCL) block, determined from ^{13}C NMR signal integrals (Equation 3 and Figure S4); [c] Molar fraction of VAc in the P(VAc-*co*-VCL) block, determined from ^{1}H NMR signal integrals (Equation 2 and Figure S3b); [d] X_m is the overall monomer molar conversion at 5h30 min of polymerization determined by ^{1}H NMR (Equation 1); [e] Theoretical number-average molar mass from Equation 4; [f] Values obtained from the SEC analysis with a MALLS detector using the d*n*/d*c* values given in experimental part; [g] Number-average hydrodynamic diameter of PEG-*b*-P(VAc-*co*-VCL) copolymer dispersions (0.5 g.L^{-1}), measured at 55 °C at the end of the reaction (without cooling), corresponding to 98 % and 91 % of the intensity signal for Expt 1 and Expt 2 respectively.

For the sake of comparison, emulsion copolymerization of VAc and VCL with an initial molar fraction of VAc equals to 0.5 ($f_{VAc,0}$ = 0.5) was carried out using a non-reactive PEG-OH hydrophilic polymer as the sole stabilizer (expt 3 in **Table 1**). The growing polymer spontaneously precipitated during the emulsion copolymerization of VAc and VCL to produce a large coagulum

representing 97 wt-% of the polymer (**Figure S5**). These results highlighted the crucial role played by the reactive xanthate chain-end of PEG-X during the emulsion polymerization process, ensuring the colloidal stability of the particles by means of the *in-situ* synthesis and self-assembly of amphiphilic PEG-*b*-P(VAc-*co*-VCL) block copolymers. Indeed, as displayed in **Figure 1** and **Figure S6**, the shift of the SEC chromatograms towards lower elution volumes suggests that the PEG-X was chain extended by the P(VAc-*co*-VCL) block.

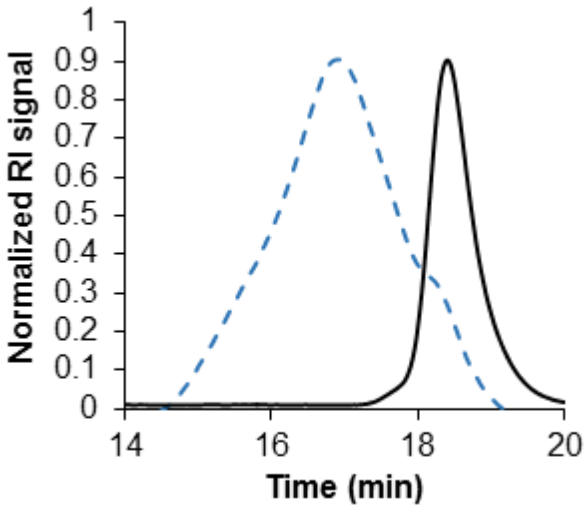

Figure 1. Size exclusion chromatograms in THF: PEG-X (full line) and PEG-*b*-P($VAc_{0.47}$-*co*-$VCL_{0.53}$) copolymer synthesized by RAFT/MADIX emulsion polymerization (expt 2 in **Table 2**).

The chromatograms of the final block copolymers display a shoulder that can be ascribed to an incomplete consumption of the initial macromolecular PEG-X chain transfer agent as suggested by Binauld *et al.*[25] for RAFT/MADIX emulsion polymerization of VAc mediated by a xanthate-functionalized PEG. The incomplete consumption of the macromolecular RAFT agent is at the origin of lower values of experimental M_n compared to theoretical M_n of the block copolymers as the residual low molar mass PEO is accounted in the average experimental M_n (**Table 2**). The low efficiency of xanthate was also observed for bulk VAc/VCL copolymerization mediated by a molecular xanthate agent.[54] In order to assess the effective formation of the PEG-*b*-P(VAc-*co*-VCL) block copolymers by emulsion polymerization, the final dialyzed samples were analyzed by DOSY NMR spectroscopy. This technique allows for the identification of different components in the mixture by means of the acquisition of two-dimensional spectra which correlate the diffusion

coefficient of each component with their corresponding chemical shifts.[58] As depicted in **Figure 2** and **Figure S7**, the signals corresponding to PEG and P(VAc-*co*-VCL) blocks are aligned with one diffusion coefficient, which confirms that both blocks are part of the block copolymer structure. DOSY NMR spectra also show the presence of residual unreacted PEG homopolymer with higher diffusion coefficient of 86 $\mu m^2.s^{-1}$. The diffusion coefficient of PEG-*b*-P($VAc_{0.47}$-*co*-$VCL_{0.53}$) is slightly lower (D = 36 $\mu m^2.s^{-1}$) than the PEG-*b*-P($VAc_{0.17}$-*co*-$VCL_{0.83}$) (D = 45 $\mu m^2.s^{-1}$) according to the higher M_n of the more hydrophobic copolymer (see **Table 2**).

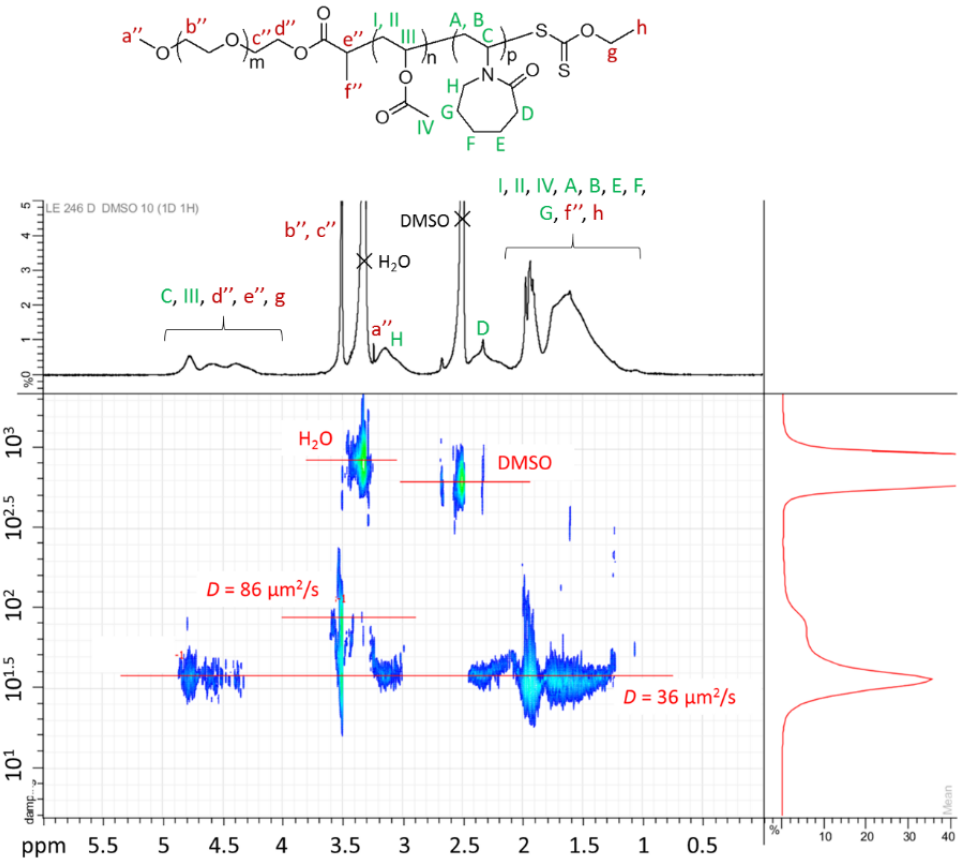

Figure 2. DOSY NMR spectrum in DMSO-d_6 of the dialyzed PEG-*b*-P($VAc_{0.47}$-*co*-$VCL_{0.53}$) copolymer synthesized by RAFT/MADIX emulsion polymerization (expt 2 in **Table 2**).

In comparison with the low dispersity values of the statistical P(VAc-*co*-VCL) copolymers synthesized in bulk ($Đ$ < 1.3),[54] the dispersity values of the PEG-*b*-P(VAc-*co*-VCL) copolymers synthesized by emulsion copolymerization are higher ($Đ$ = 1.6 – 2.0) (see **Table 2**). The presence of unreacted PEG is at the origin of the higher dispersity values. Also, the higher concentration of VCL water solubility limit in comparison with VAc ($[VCL]_{limit,\ water,\ 25°C}$ = 41 $g.L^{-1}$, $[VAc]_{limit,\ water,}$

$_{20°C}$ = 23 g.L^{-1}),[1, 59] might induce the enrichment in VCL for the initial growing oligomer chains produced in the water phase. It was concluded from our previous work carried out in bulk that dispersity values of P(VAc-*co*-VCL) statistical copolymers increases with increasing the initial VCL feed ratio.[54] The final average composition of the P(VAc-*co*-VCL) block was calculated by proton and carbon NMR (**Figure S3** and **Figure S4**). The determination of the copolymer composition by comparing the integrals of both carbonyls of the ^{13}C NMR spectrum corresponding to each polymer units is of interest because of the good level of resolution. These compositions match those determined from the integrals of ^{1}H NMR spectrum of the PEG-*b*-P(VAc-*co*-VCL) (**Table 2**). The ^{13}C NMR analysis of both PEG-*b*-P(VAc$_{0.17}$-*co*-VCL$_{0.83}$) and PEG-*b*-P(VAc$_{0.47}$-*co*-VCL$_{0.53}$) copolymers also shows that the shapes of the characteristic methine signals of both PVAc ($CH_{II'}$, 65 – 70 ppm) and PVCL units ($CH_{B'}$, 45 – 49 ppm) are influenced by the copolymer composition (**Figure 3**). Indeed, it is known that the probability of the different co-monomer triads in a statistical copolymer, depending among other factors to the initial monomer feed ratio, influences the chemical environment of each monomer unit.

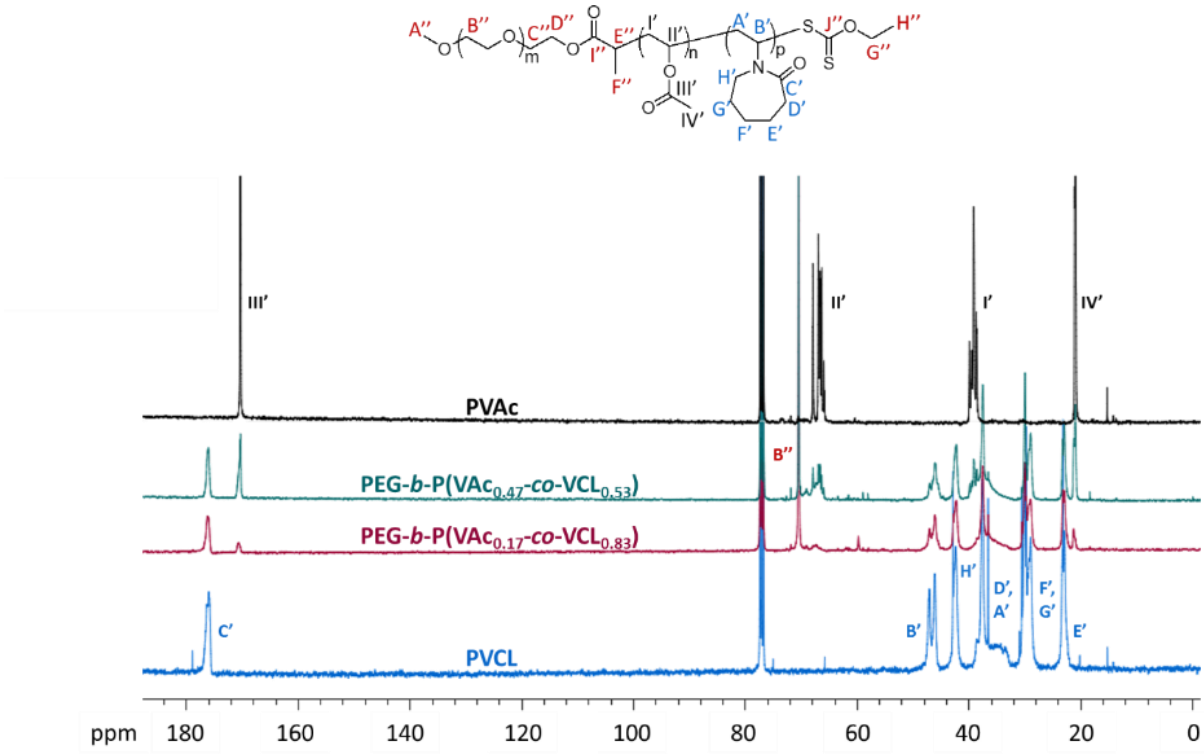

Figure 3. Overlay of the ^{13}C NMR spectra of the precipitated PVAc, PVCL, PEG-*b*-P(VAc$_{0.17}$-*co*-VCL$_{0.83}$) and PEG$_{49}$-P(VAc$_{0.47}$-*co*-VCL$_{0.53}$) (co)polymers in $CDCl_3$.

The ^{13}C NMR spectra of the PEG-*b*-P(VAc-*co*-VCL) copolymers synthesized by emulsion polymerization were compared with the ones of their P(VAc-*co*-VCL) counterparts of similar composition synthesized in bulk. The signals of both PVAc and PVCL units exhibiting a similar shape between bulk and emulsion copolymers of similar composition ($CH_{II'}$, $CH_{B'}$ in **Figure S8**), the distribution of the co-monomer along the chain probably follows a similar statistic. The additional small peaks observed for the PEG-*b*-P(VAc-*co*-VCL) copolymers in the range of 50 to 75 ppm arise from the chain end signals of the PEG-xanthate (A", D", C") and from the rotational bands of the main PEO peak (B").

The pictures of the dispersion of PEG-*b*-P(VAc-*co*-VCL) particles displayed in **Figure 4** show a macroscopic observation of the latex at different temperatures (T = 5°C, 20°C and at 50°C). The latex produced at 65°C was cooled at 5 °C followed by a gradual heating up to 20°C and 50°C. The PEG-*b*-P($VAc_{0.47}$-*co*-$VCL_{0.53}$) copolymer synthesized by emulsion polymerization is a white dispersion of diffusing particles in the whole range of temperatures while translucent aqueous solutions of PEG-*b*-P($VAc_{0.17}$-*co*-$VCL_{0.83}$) were observed at 5°C (**Figure 4**). This suggests that a sufficient level of hydrophobic interactions between the VAc units (47 mol-%) is enable to preserve the integrity of the PEG-*b*-P($VAc_{0.47}$-*co*-$VCL_{0.53}$) particles even at low temperature. The dispersion of PEG-*b*-P($VAc_{0.17}$-*co*-$VCL_{0.83}$) copolymer in water becomes gradually cloudier by increasing the temperature (LE 245, **Figure 4**), which is the sign of thermo-induced increasing size of the diffusing objects.

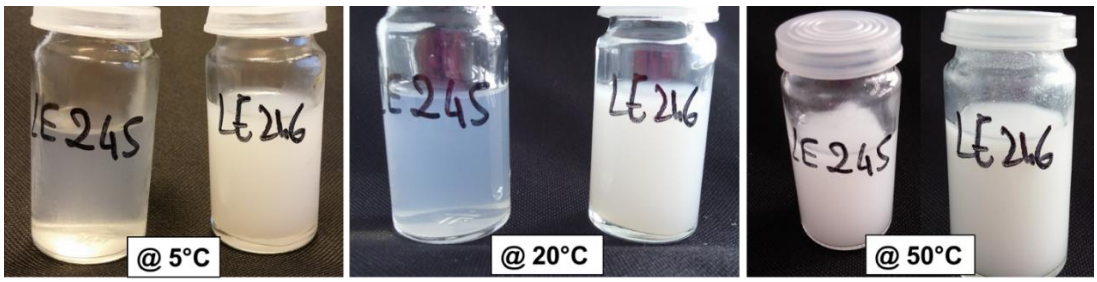

Figure 4. Pictures taken at different temperatures (5°C, 20°C and 50°C) of the final polymer dispersion obtained by PEG-X mediated emulsion copolymerization of VAc and VCL. For each picture, left sample corresponds to: PEG-*b*-P($VAc_{0.17}$-*co*-$VCL_{0.83}$) copolymer (Expt 1 in **Table 1,** LE245) and right sample corresponds to PEG-*b*-P($VAc_{0.47}$-*co*-$VCL_{0.53}$) copolymer (Expt 2 in **Table 1,** LE246).

Turbidimetry is a suitable method to monitor the thermoresponsiveness of the PEG-*b*-P(VAc-*co*-VCL) block copolymers synthesized by emulsion copolymerization. The evolution of

transmittance versus temperature of the different copolymers is displayed in **Figure 5** and the experimental values of the phase transition temperature are gathered in **Table 3**.

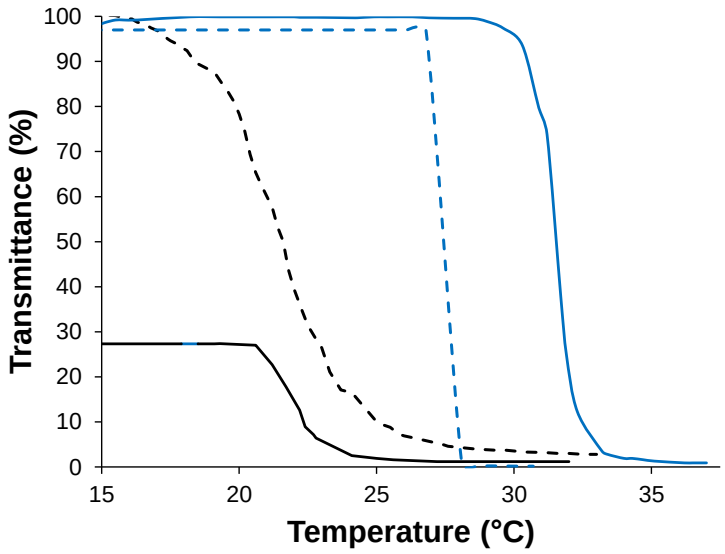

Figure 5. Transmittance at λ = 500 nm versus temperature for aqueous solution of PEG-*b*-P(VAc-*co*-VCL) copolymers synthesized by RAFT/MADIX emulsion polymerization (plain lines, present work): PEG-*b*-P($VAc_{0.17}$-*co*-$VCL_{0.83}$) (blue) and PEG-*b*-P($VAc_{0.47}$-*co*-$VCL_{0.53}$) (black). Comparison with transmittance of P(VAc-*co*-VCL) copolymers with similar compositions synthesized by RAFT/MADIX bulk polymerization from reference 54 (dotted lines): P($VAc_{0.19}$-*co*-$VCL_{0.81}$) (blue) and P($VAc_{0.53}$-*co*-$VCL_{0.47}$). Polymer concentration of 3 $g.L^{-1}$ (heating cycle).

Table 3. Phase transition temperatures of PEG-*b*-P(VAc-*co*-VCL) copolymers synthesized by emulsion polymerization.

Expt	Copolymer	F_{VAc}	PTT, UV-vis[a] °C
1	PEG-*b*-P($VAc_{0.17}$-*co*-$VCL_{0.83}$)	0.17	32
2	PEG-*b*-P($VAc_{0.47}$-*co*-$VCL_{0.53}$)	0.47	22

[a] Phase transition temperature, see **Figure 5**.

The solution of PEG-*b*-P($VAc_{0.17}$-*co*-$VCL_{0.83}$) copolymer allows for 100 % of light transmittance at low temperatures, which is in accordance with the absence of large diffusing objects below the phase transition temperature (**Figure 4** and **Figure 5**). On the other hand, the 28 % transmittance of the aqueous dispersion of PEG-*b*-P($VAc_{0.47}$-*co*-$VCL_{0.53}$) copolymer observed at low temperature is consistent with the presence of stable diffusing particles even at low temperature by means of sufficient hydrophobic interactions between VAc units (**Figure 4** and **Figure 5**). The more

hydrophobic PEG-*b*-P($VAc_{0.47}$-*co*-$VCL_{0.53}$) exhibits a lower phase transition temperature than the PEG-*b*-P($VAc_{0.17}$-*co*-$VCL_{0.83}$) as the enhanced hydrophobic interactions promotes the polymer collapse (**Table 3**). Note that the hydrophobic xanthate chain-end of the PEG-X does not impart any phase transition temperature to the low molar mass PEG as no variation of the transmittance was observed in the temperature range of 20 to 75°C (**Figure S9**). The presence of the hydrophilic PEG sequence in the PEG-*b*-P($VAc_{0.17}$-*co*-$VCL_{0.83}$) copolymer influences the thermal response of the P($VAc_{0.17}$-*co*-$VCL_{0.83}$) sequence as a shift towards a higher phase transition temperature (PTT = 32 °C) is observed in comparison to the P($VAc_{0.19}$-*co*-$VCL_{0.81}$) statistical copolymer of close composition (PTT = 27°C). On the other hand, the similar values of the phase transition temperatures (PTT = 22°C) of both PEG-*b*-P($VAc_{0.47}$-*co*-$VCL_{0.53}$) and P($VAc_{0.53}$-co-$VCL_{0.47}$) copolymers with higher VAc fraction traduces a predominant effect of these hydrophobic units on the collapse of the thermoresponsive copolymer chains. The hydrodynamic diameters of the particles synthesized by VAc/VCL emulsion copolymerization carried out in the presence of the PEG-X stabilizer were measured at 55 °C directly at the end of the polymerization process, without cooling the reaction medium (**Table 2**). The average hydrodynamic diameter of the PEG-*b*-P($VAc_{0.47}$-*co*-$VCL_{0.53}$) particles (D_h = 95 nm) is lower than the one of PEG-*b*-P($VAc_{0.17}$-*co*-$VCL_{0.83}$) particles (D_h = 150 nm), thus indicating a higher number of particles for the highest initial fraction of hydrophobic monomer ($f_{VAc,0}$ = 0.5). The increasing hydrophobicity likely results in the early self-assembly of the PEG-*b*-P(VAc-*co*-VCL) copolymer synthesized during the nucleation step, hence producing a higher number of particles. We further investigated the thermoresponsive behavior of the PEG-*b*-P(VAc-*co*-VCL) copolymers synthesized by emulsion copolymerization. For that purpose, the aqueous dispersions of the amphiphilic copolymers were cooled down at room temperature after the polymerization process to be subsequently analyzed by dynamic light scattering. A heating and cooling cycle was applied in the range of 10°C to 55°C, at a polymer concentration of 0.05 $g.L^{-1}$ (**Figure 6**). The temperature-dependence of the hydrodynamic diameters confirms the occurrence of a thermoresponsive phase transition for both types of copolymer particles but with opposite profiles (**Figure 6**).

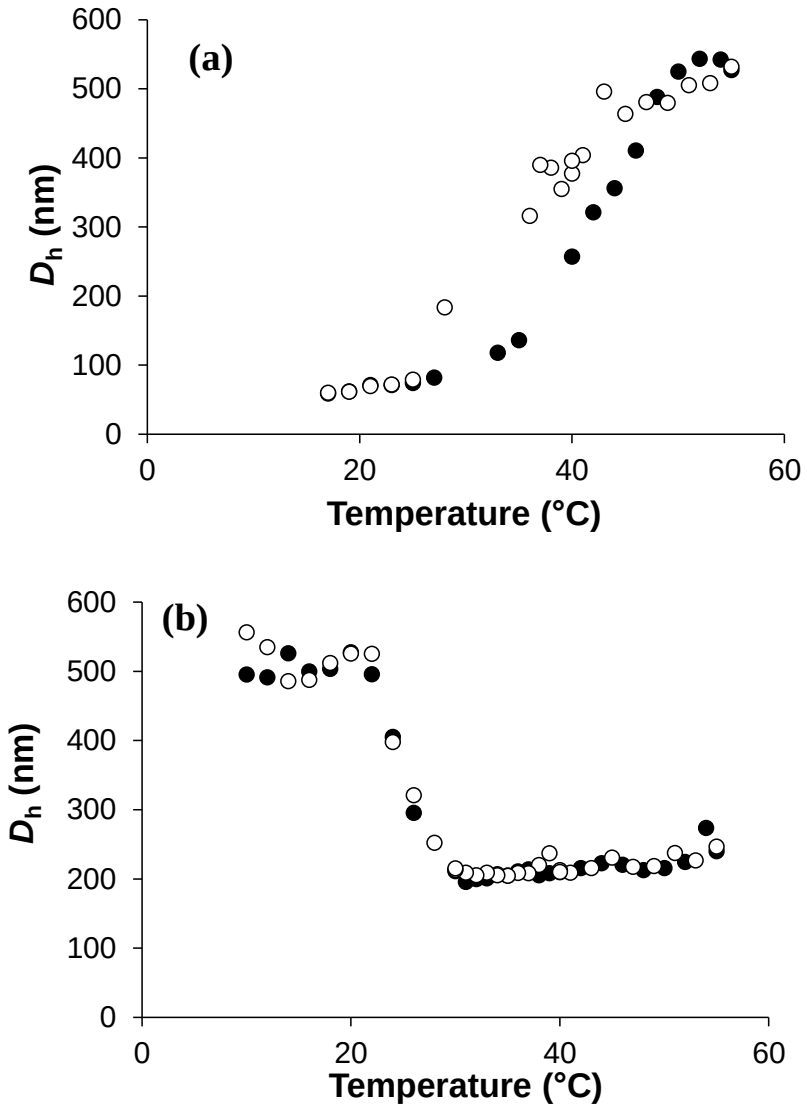

Figure 6. Hydrodynamic diameters as a function of the temperature for the PEG-*b*-P(VAc-*co*-PVCL) dispersions synthesized by emulsion polymerization at 10 wt-% of initial solids content for different initial monomer feed ratio **(a)** F_{VAc} = 0.17 (expt 1 in **Table 1**) and **(b)** F_{VAc} = 0.47 (expt 2 in **Table 1**). (●) 1st heating cycle, (○) cooling cycle of polymer dispersions at 0.05 g.L^{-1}.

Indeed, the D_h versus temperature profile for PEG-*b*-P(VAc$_{0.17}$-*co*-VCL$_{0.83}$) copolymer (expt 1 in **Table 1**) (**Figure 6a**) is close to the one of the (PVAc-*co*-PVCL) statistical copolymers synthesized in bulk (see reference [54]) in the sense that D_h increases by rising temperature. The very low average count rate measured at low temperature, quantifying the diffused light intensity, suggests that PEG-*b*-P(VAc$_{0.17}$-*co*-VCL$_{0.83}$) copolymer chains disassembled into very small objects of 50 nm in water at a temperature below 20°C. The presence of objects with diameter of *ca* 600 nm above the phase

transition temperature, together with the hysteresis observed between heating and cooling cycles, both support the formation of polydisperse aggregates of the PEG-*b*-P($VAc_{0.17}$-*co*-$VCL_{0.83}$) copolymer chains by increasing temperature up to 55°C (**Figure 6a**). Note that the self-assembly induced by dehydration of the hydrophobic PVCL block has been previously investigated for PEG-*b*-PVCL diblock copolymers.[55] Despite the balanced compositions between the hydrophilic and hydrophobic blocks, these PEG_{114}-*b*-PVCL*x* diblock copolymers self-assembled into large aggregates (D_h ~ 300 to 550 nm) instead of well-defined micelles.[55] Contrary to PEG-*b*-P($VAc_{0.17}$-*co*-$VCL_{0.83}$) copolymer, emulsion copolymerization of VAc/VCL performed with 50 mol-% of VAc in the initial monomer feed (expt 2 in **Table 1**) produced stable particles at low temperature by means of sufficient hydrophobic interactions between the VAc units ($D_{h,\ 10\text{-}20°C}$ = 550 nm) (**Figure 6b**). The collapse of the P($VAc_{0.47}$-*co*-$VCL_{0.53}$) blocks within the particles by increasing temperature induced a decrease of the particle diameter down to 250 nm at 55°C. The reversible swelling-to-collapse transition of the PEG-*b*-P($VAc_{0.47}$-*co*-$VCL_{0.53}$) particles with almost no hysteresis emphasizes the formation of well-defined physically crosslinked thermoresponsive particles of P($VAc_{0.47}$-*co*-$VCL_{0.53}$) stabilized by the PEG block (**Figure 6b**). The volume phase transition temperature (VPTT) of the PEG-*b*-P($VAc_{0.47}$-*co*-$VCL_{0.53}$) particles, determined as the minimum of the derivative of the plot of D_h as a function of the temperature, is equal to 26°C at 0.05 $g.L^{-1}$. The slightly higher value of VPTT measured by DLS at 0.05 $g.L^{-1}$ (**Figure 6**) in comparison with the phase transition temperature of PEG-*b*-P($VAc_{0.47}$-*co*-$VCL_{0.53}$) copolymer (PTT = 22 °C, **Figure 5**) measured by turbidimetry at 3 $g.L^{-1}$ shows a concentration effect on the transition temperature. The VPTT of the PEG-*b*-P($VAc_{0.47}$-*co*-$VCL_{0.53}$) particles is lower than the one measured for chemically crosslinked PVCL-based nanogels (~32°C),[42, 60-62] due to the presence of the VAc hydrophobic units. Indeed, as the hydrophobic composition of thermoresponsive copolymers is increased, the hydrogen bonding effect between the copolymer chains and water is lowered while hydrophobic interactions are enhanced, thus lowering the required energy to collapse.[50, 51] It should be noticed that the D_h of the collapsed particles measured after applying a cooling/heating cycle to the PEG-*b*-P($VAc_{0.47}$-*co*-$VCL_{0.53}$)$_4$ particle dispersion ($D_{h,\ 55°C}$ = 250 nm) is higher than the one measured for the kinetically-trapped particles recovered at the end of the polymerization at 55 °C in the absence of any cooling step ($D_{h,\ 55°C}$ = 95 nm) (**Table 2**). After cooling the latex, some PEG-*b*-P($VAc_{0.47}$-*co*-$VCL_{0.53}$) copolymer chains might exchange between the swollen particles formed by hydrophobic interactions, thus producing particles of larger size.

Such difference between the D_h measured at high temperature at the end of polymerization or after a cooling step has already been observed for physically crosslinked thermoresponsive particles synthesized by PISA.[37] In a recent study, *in situ* time-resolved SAXS measurements monitoring particles synthesized by RAFT PISA revealed an increase of the mean aggregation number as a function of monomer conversion for the kinetically-trapped spheres.[63] As perspective, the presence of the hydrophobic PVAc within the physically crosslinked particles might be of interest to enhance the loading capacity of hydrophobic molecules.

Alkaline hydrolysis of the PEG-*b*-P(VAc-*co*-VCL)

Poly(vinyl alcohol) (PVA) is prepared upon alkaline hydrolysis of PVAc under mild conditions (transesterification with methanol) leading to PVA with different degrees of saponification.[53, 64] It has been shown that a degree of saponification of 88 % was optimum to provide a water soluble polymer as the hydrophobic acetyl neighborhood limits the hydrogen bonding between poly(vinyl alcohol) chains.[53] Therefore, the P(VAc-*co*-VCL)-based copolymers directly synthesized in water by emulsion polymerization are potential precursors of P(VA-*co*-VCL) copolymers. This is a strategy to synthesize by an environmentally friendly process some biocompatible thermoresponsive statistical copolymers with a tunable phase transition. The efficiency of the alkaline hydrolysis of PEG-*b*-P(VAc-*co*-VCL) copolymers was monitored by ^{1}H NMR analysis of the copolymers before and after hydrolysis (**Figure 7** and **Figure S10**). For both copolymers, the effective hydrolysis was attested by the appearance of the PVA characteristic signals at 3.8 - 4.5 ppm (*N* and *M* protons) together with the disappearance of PVAc signals at 4.8 ppm (*III* methyne proton) and 1.8 ppm (*IV* methyl protons) (**Figure 7** and **Figure S10)**.

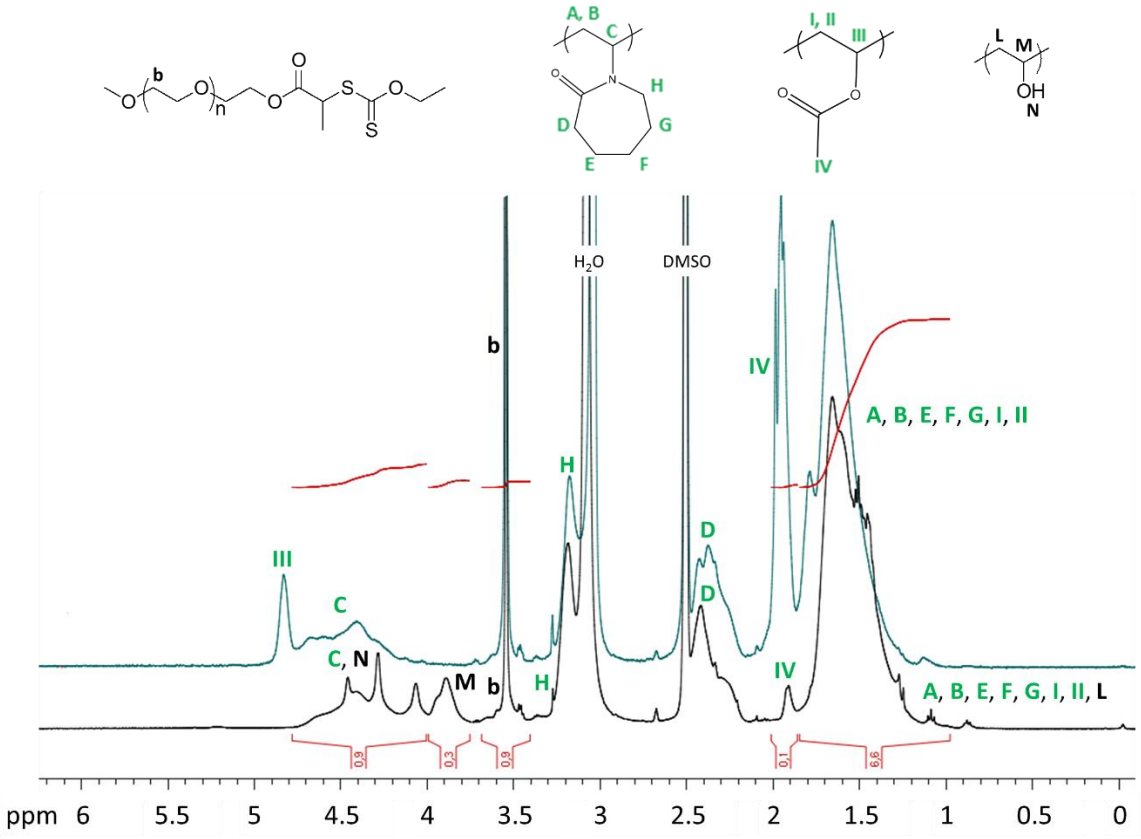

Figure 7. ^{1}H NMR spectra in DMSO-d_6 at 80°C of the dialyzed and freeze-dried PEG-*b*-P(VAc$_{0.47}$-*co*-VCL$_{0.53}$) (expt 2 in **Table 1**) copolymer (blue) and of the corresponding copolymer after hydrolysis (black).

The yield of hydrolysis of the copolymers can be calculated on the basis of the integrations of the characteristic NMR peaks of PVA and PVAc units (Equation 5).

$$\%\ hydrolysis = \frac{n_{PVOH}}{n_{PVOH} + n_{PVAc}} = 1 - \frac{\frac{I_{1HPVAc,after\ hydrolysis}}{I_{reference}}}{\frac{I_{1HPVAc,after\ hydrolysis}}{I_{reference}} + \frac{I_{1HPVAc,before\ hydrolysis}}{I_{reference}}} \quad \text{Equation 5}$$

$I_{1\text{HPVAc, before hydrolysis}}$ and $I_{1\text{HPVAc, after hydrolysis}}$ were obtained from the integral of *IV* protons of PVAc before and after hydrolysis and $I_{\text{reference}}$ corresponds to the integral of the signal between 1.0 and 1.8 ppm (**Figure 7**). The hydrolysis yields calculated from Equation 5 are given in **Table 4**.

Table 4. Hydrolysis yields (in %) of PEG-*b*-P(VAc-*co*-VCL) copolymers.

% hydrolysis	FTIR	^{1}H NMR	Average % of hydrolysis
PEG-*b*-P(VAc$_{0.17}$-*co*-VCL$_{0.83}$)	77	87	82 ± 7
PEG-*b*-P(VAc$_{0.47}$-*co*-VCL$_{0.53}$)	85	94	90 ± 6

The hydrolysis of the PVAc units of the PEG-*b*-P(VAc-*co*-VCL) copolymers was also monitored by Fourier Transform Infra-Red (FTIR) spectroscopy via the disappearance of the characteristic ester band of the PVAc at 1730 cm^{-1} (**Figure 8** and **Figure S11**). Through a normalization with the signal of the amide bond of PVCL units of copolymers before and after hydrolysis, the yield of hydrolysis was calculated by comparing the absorbance of the ester band of PVAc (1730 cm^{-1}) before and after the hydrolysis step. The range of hydrolysis yield calculated by FTIR is slightly lower (77-85 %) in comparison with the yield calculated by NMR (87-94 %) but in a similar range to provide an average yield of hydrolysis (see **Table 4**). The shift of the PVCL amide resonance frequency from 1623 cm^{-1} in the initial PEG-*b*-P($VAc_{0.47}$-*co*-$VCL_{0.53}$) copolymer to 1604 cm^{-1} in the hydrolyzed copolymer traduces the surrounding change from PVAc to PVA neighbor units (**Figure 8**). The normalization of the absorption band at 2850 – 2950 cm^{-1} characteristic of the aliphatic carbon stretching shows a constant intensity of the amide band of PVCL (1604 - 1623 cm^{-1}) before and after hydrolysis, which excludes any concomitant PVCL hydrolysis.

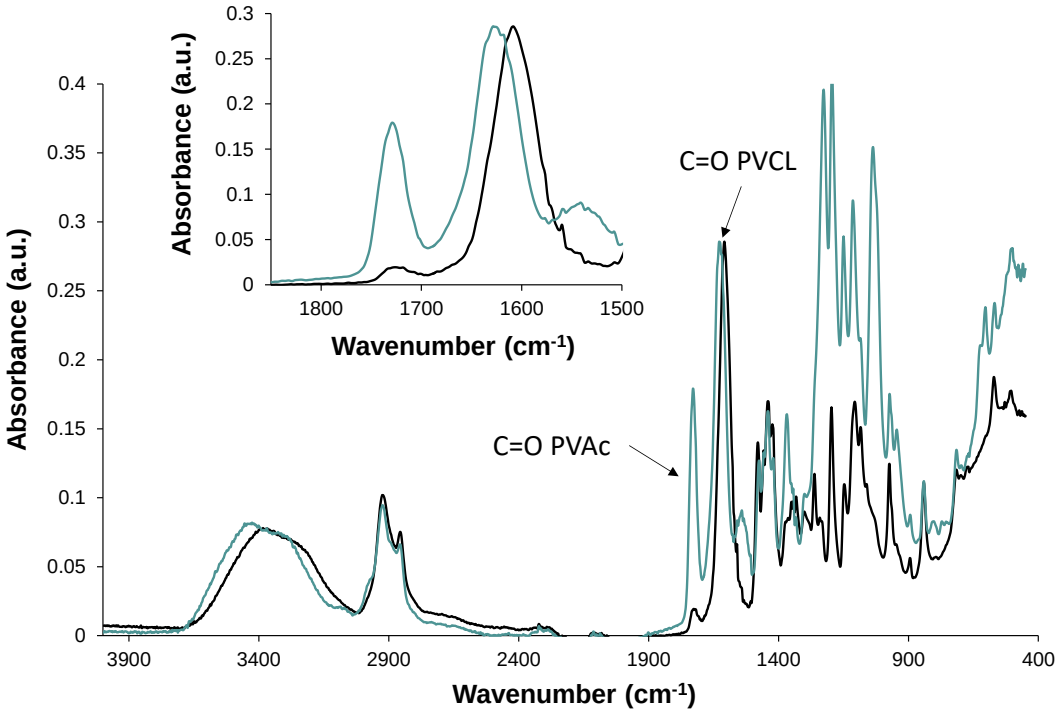

Figure 8. FTIR spectra before (blue) and after hydrolysis (black) of PEG-*b*-P($VAc_{0.47}$-*co*-$VCL_{0.53}$) copolymer.

These results show that is it possible to produce thermoresponsive P(VAc-*co*-VA-*co*-VCL) copolymers of controlled molar mass from the PEG-*b*-P(VAc-*co*-VCL) copolymers synthesized by surfactant-free emulsion polymerization process. The covalent linkage between the reactive PEG-xanthate and the P(VAc-*co*-VCL) block being an ester group, the analysis of the polymer after hydrolysis by DOSY NMR was required to provide information on the stability of the covalent bonding. Only one diffusion coefficient correlated to the ^{1}H NMR characteristic signals of the PEG block (I_b,, at 3.5 ppm) is observed in **Figure S12** at D = 86 µm^{2}s^{-1} corresponding to the free PEG (**Figure S7**). A better alignment of PEG and P(VAc-*co*-VCL) blocks was observed for the PEG-*b*-P(VAc-*co*-VCL) block copolymer precursors (**Figure 2** and **Figure S7**). Therefore, DOSY-NMR analyses evidence the hydrolysis of the covalent linkage between both PEG and P(VAc-*co*-VA-*co*-VCL) blocks. Note that an average weight fraction of 6 wt-% of residual PEO versus the total mass of polymer was calculated by proton NMR for both copolymers (see example in Figure 7).

The thermoresponsive behavior of the P(VAc-*co*-VA-*co*-PVCL) copolymers in water was investigated by means of DLS measurements. The increase of the hydrodynamic diameter by increasing the temperature confirms the thermoresponsive behavior in water of both P(VAc-*co*-VA-*co*-VCL) copolymers with a phase transition temperature ranging between 26°C and 30°C (**Figure 9**).

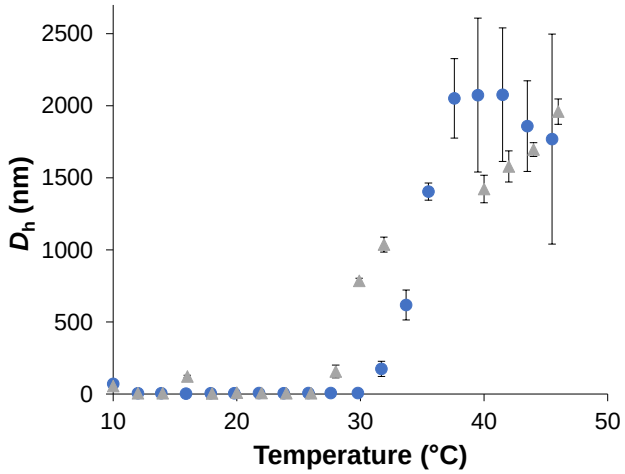

Figure 9. Evolution of the hydrodynamic diameter of the P(VAc-*co*-VA-*co*-VCL) copolymers a function of the temperature: (●) P(VAc$_{0.03}$-*co*-VA$_{0.14}$-*co*-VCL$_{0.83}$) copolymer, (▲) P(VAc$_{0.05}$-*co*-VA$_{0.42}$-*co*-VCL$_{0.53}$) copolymer at 5 g.L^{-1} in water (heating cycle).

As a perspective of this work, as poly(vinyl alcohol) is known to be a biodegradable polymer under suitable conditions,[53] it would be of interest to investigate how the incorporation of PVA units into the biocompatible PVCL copolymer particles might provide degradable linkages in order to produce more attractive thermoresponsive degradable PVCL-based materials.[65]

CONCLUSION

In conclusion of this work, the RAFT/MADIX batch emulsion copolymerization of vinyl acetate (VAc) and *N*-vinylcaprolactam (VCL) mediated by a xanthate-terminated PEG macromolecular chain-transfer agent was successfully performed at 10 wt-% of solids content, with two different initial monomer feed ratios. DOSY NMR and SEC analyses both support the successful chain extension of the PEG-X macro-CTA enabling the direct synthesis and self-assembly of thermoresponsive PEG-*b*-P(VAc-*co*-VCL) block copolymers in aqueous dispersed media. The present study is the first example of synthesis of PVCL-based amphiphilic copolymers by controlled radical emulsion polymerization. It is worth to mention that the PEG-X efficiently acted as both steric stabilizer and macromolecular chain-transfer agent during the RAFT/MADIX emulsion copolymerization of VAc and VCL to produce well-defined physically crosslinked thermoresponsive particles via hydrophobic interactions between the self-assembled PEG-*b*-P(VAc-*co*-VCL) copolymers. The integrity of the particles at a temperature below the phase transition temperature is maintained by means of hydrophobic interactions with 47 mol-% of hydrophobic VAc units in the P(VAc-*co*-VCL) sequence of the block copolymer. The well-defined physically crosslinked PEG-*b*-P($VAc_{0.47}$-*co*-$VCL_{0.53}$) particles interestingly behaved as thermoresponsive colloids able to undergo a reversible swelling-to-collapse transition upon increasing the temperature. A lower fraction of VAc in the copolymer (17 mol-%) was not sufficient to prevent disassembling of the PEG-*b*-P($VAc_{0.17}$-*co*-$VCL_{0.83}$) polymer chains in the aqueous phase at low temperature ($T < 20°C$). The PEG-*b*-P($VAc_{0.17}$-*co*-$VCL_{0.83}$) copolymer chains self-assemble into large polydisperse aggregates by rising the temperature. Finally, the VAc/VCL statistical copolymers of controlled molar mass were successfully hydrolyzed into promising thermoresponsive biocompatible statistical copolymers based on vinyl alcohol and *N*-vinylcaprolactam units.

ACKNOWLEDGEMENTS

The French ministry of research, the University of Pau & Pays Adour and the University of the Basque Country UPV/EHU are acknowledged for funding L.E.'s PhD work performed under a joint doctorate program. The Equipex Xyloforest program (ANR-10-EQPX-16 XYLOFOREST) is acknowledged for MALLS detector and NMR probe funding. Prof. P. Stepanek is acknowledged for giving us the opportunity to perform measurements with the Zetasizer Nano ZS instrument at the institute of macromolecular chemistry (Prague).

Electronic supplementary information (ESI) available: Preparation of PEG-X macro-chain transfer agent and ^{1}H NMR spectra; Overlay of the UV-visible (λ = 355 nm) and refractometer (RI) traces of the SEC chromatograms in THF for the PEG-X polymer; ^{1}H NMR and ^{13}C NMR spectra of the dialyzed and freeze-dried PEG-*b*-P(VAc-*co*-VCL) diblock copolymers; Pictures of the coagulum and of the dispersion recovered at the end of the emulsion copolymerization of VAc and VCL using non-reactive PEG-OH as stabilizer; Size exclusion chromatograms of PEG-X and PEG-*b*-P($VAc_{0.17}$-*co*-$VCL_{0.83}$) copolymer; DOSY NMR spectra of the dialyzed PEG-*b*-P($VAc_{0.17}$-*co*-$VCL_{0.83}$) copolymer and initial PEG-OH homopolymer; Comparison of ^{13}C NMR spectra of the VAc/VCL copolymers synthesized either by bulk polymerization or by emulsion polymerization; Transmittance at λ=500 nm versus temperature for aqueous solution of PEG-X; ^{1}H NMR spectra before and after hydrolysis of PEG-*b*-P($VAc_{0.17}$-*co*-$VCL_{0.83}$) copolymer; FTIR spectra before and after hydrolysis of PEG-*b*-P($VAc_{0.17}$-*co*-$VCL_{0.83}$) copolymer; DOSY NMR spectrum of PEG-*b*-P($VAc_{0.03}$-*co*-$VA_{0.14}$-*co*-$VCL_{0.83}$) and PEG-*b*-P($VAc_{0.05}$-*co*-$VA_{0.42}$-*co*-$VCL_{0.53}$) copolymers after hydrolysis.

REFERENCES

1. M. J. Barandiaran, J. C. Cal and J. M. Asua, in *Polym. React. Eng.*, Blackwell Publishing Ltd, 2008, pp. 233-272.
2. E. Gil and S. Hudson, *Prog. Polym. Sci.*, 2004, **29**, 1173-1222.
3. M. A. Stuart, W. T. Huck, J. Genzer, M. Muller, C. Ober, M. Stamm, G. B. Sukhorukov, I. Szleifer, V. V. Tsukruk, M. Urban, F. Winnik, S. Zauscher, I. Luzinov and S. Minko, *Nat Mater*, 2010, **9**, 101-113.
4. D. Roy, W. L. Brooks and B. S. Sumerlin, *Chem Soc Rev*, 2013, **42**, 7214-7243.

5. J. M. Hu, M. R. Whittaker, Y. Li, J. F. Quinn and T. P. Davis, *Polym. Chem.*, 2015, **6**, 2407-2415.
6. M. R. Islam and M. J. Serpe, *Macromolecules*, 2013, **46**, 1599-1606.
7. J. M. Weissman, H. B. Sunkara, A. S. Tse and S. A. Asher, *Science*, 1996, **274**, 959-960.
8. B. P. Tripathi, N. C. Dubey and M. Stamm, *Acs Applied Materials & Interfaces*, 2014, **6**, 17702-17712.
9. Z. Mouline, M. Semsarilar, A. Deratani and D. Quemener, *Polym. Chem.*, 2015, **6**, 2023-2028.
10. C. de Las Heras Alarcon, S. Pennadam and C. Alexander, *Chem Soc Rev*, 2005, **34**, 276-285.
11. A. S. Hoffman, *Adv Drug Deliv Rev*, 2013, **65**, 10-16.
12. S. Nayak and L. A. Lyon, *Angew Chem Int Ed Engl*, 2005, **44**, 7686-7708.
13. N. M. B. Smeets and T. Hoare, *J. Polym. Sci., Part A: Polym. Chem.*, 2013, **51**, 3027-3043.
14. B. R. Saunders, N. Laajam, E. Daly, S. Teow, X. Hu and R. Stepto, *Adv Colloid Interface Sci*, 2009, **147-148**, 251-262.
15. P. B. Zetterlund, Y. Kagawa and M. Okubo, *Chem. Rev.*, 2008, **108**, 3747-3794.
16. P. B. Zetterlund, S. C. Thickett, S. Perrier, E. Bourgeat-Lami and M. Lansalot, *Chem. Rev.*, 2015, **115**, 9745-9800.
17. M. J. Monteiro and M. F. Cunningham, *Macromolecules*, 2012, **45**, 4939-4957.
18. R. W. Simms, T. P. Davis and M. F. Cunningham, *Macromol. Rapid Commun.*, 2005, **26**, 592-596.
19. J. P. Russum, N. D. Barbre, C. W. Jones and F. J. Schork, *J. Polym. Sci., Part A: Polym. Chem.*, 2005, **43**, 2188-2193.
20. B. Jiang, Q. H. Zhang, X. L. Zhan and F. Q. Chen, *Chin. Chem. Lett.*, 2009, **20**, 733-737.
21. C. Detrembleur, A. Debuigne, R. Bryaskova, B. Charleux and R. Jérôme, *Macromol. Rapid Commun.*, 2006, **27**, 37-41.
22. F. Zhao, A. R. Mahdavian, M. B. Teimouri, E. S. Daniels, A. Klein and M. S. El-Aasser, *Colloid. Polym. Sci.*, 2012, **290**, 1247-1255.
23. N. Nomura, K. Shinoda, A. Takasu, K. Nagata and K. Inomata, *J. Polym. Sci., Part A: Polym. Chem.*, 2013, **51**, 534-545.
24. J. Bernard, M. Save, B. Arathoon and B. Charleux, *J. Polym. Sci., Part A: Polym. Chem.*, 2008, **46**, 2845-2857.
25. S. Binauld, L. Delafresnaye, B. Charleux, F. D'Agosto and M. Lansalot, *Macromolecules*, 2014, **47**, 3461-3472.
26. Z. Huang, P. Pan and Y. Bao, *J. Polym. Sci., Part A: Polym. Chem.*, 2016, **54**, 2092-2101.
27. N. A. Cortez-Lemus and A. Licea-Claverie, *Prog. Polym. Sci.*, 2016, **53**, 1-51.
28. B. Charleux, G. Delaittre, J. Rieger and F. D'Agosto, *Macromolecules*, 2012, **45**, 6753-6765.
29. G. Delaittre, J. Nicolas, C. Lefay, M. Save and B. Charleux, *Chem Commun (Camb)*, 2005, 614-616.
30. G. Delaittre, J. Nicolas, C. Lefay, M. Save and B. Charleux, *Soft Matter*, 2006, **2**, 223.
31. N. J. Warren and S. P. Armes, *J. Am. Chem. Soc.*, 2014, **136**, 10174-10185.
32. S. L. Canning, G. N. Smith and S. P. Armes, *Macromolecules*, 2016, **49**, 1985-2001.
33. C. A. Figg, A. Simula, K. A. Gebre, B. S. Tucker, D. M. Haddleton and B. S. Sumerlin, *Chemical Science*, 2015, **6**, 1230-1236.
34. Z. S. An, Q. H. Shi, W. Tang, C. K. Tsung, C. J. Hawker and G. D. Stucky, *J. Am. Chem. Soc.*, 2007, **129**, 14493-14499.

35. G. Delaittre, M. Save and B. Charleux, *Macromol. Rapid Commun.*, 2007, **28**, 1528-1533.
36. J. Rieger, C. Grazon, B. Charleux, D. Alaimo and C. Jerome, *Journal of Polymer Science Part a-Polymer Chemistry*, 2009, **47**, 2373-2390.
37. G. Delaittre, M. Save, M. Gaborieau, P. Castignolles, J. Rieger and B. Charleux, *Polym. Chem.*, 2012, **3**, 1526.
38. S. Chattopadhyay, E. Heine, A. Mourran, W. Richtering, H. Keul and M. Moller, *Polym. Chem.*, 2016, **7**, 364-369.
39. J. F. Lutz, O. Akdemir and A. Hoth, *J Am Chem Soc*, 2006, **128**, 13046-13047.
40. G. Vancoillie, D. Frank and R. Hoogenboom, *Prog. Polym. Sci.*, 2014, **39**, 1074-1095.
41. M. Boularas, E. Deniau-Lejeune, V. Alard, J.-F. Tranchant, L. Billon and M. Save, *Polym. Chem.*, 2016, **7**, 350-363.
42. J. Ramos, A. Imaz and J. Forcada, *Polym. Chem.*, 2012, **3**, 852-856.
43. H. Vihola, A. Laukkanen, L. Valtola, H. Tenhu and J. Hirvonen, *Biomaterials*, 2005, **26**, 3055-3064.
44. J. Liu, A. Debuigne, C. Detrembleur and C. Jerome, *Advanced Healthcare Materials*, 2014, **3**, 1941-1968.
45. A. A. Tager, A. P. Safronov, S. V. Sharina and I. Y. Galaev, *Colloid & Polymer Science*, 1993, **271**, 868-872.
46. M. Beija, J. D. Marty and M. Destarac, *Chem. Commun.*, 2011, **47**, 2826-2828.
47. Y. Yang, G. Tang, M. Hu, L. Shao, J. Li and Y. Bi, *Polymer*, 2015, **68**, 213-220.
48. A. Kermagoret, C.-A. Fustin, M. Bourguignon, C. Detrembleur, C. Jérôme and A. Debuigne, *Polym. Chem.*, 2013, **4**, 2575.
49. X. Zhao, O. Coutelier, H. H. Nguyen, C. Delmas, M. Destarac and J.-D. Marty, *Polym. Chem.*, 2015, **6**, 5233-5243.
50. H. Peng, M. Kather, K. Rübsam, F. Jakob, U. Schwaneberg and A. Pich, *Macromolecules*, 2015, **48**, 4256-4268.
51. H. Peng, W. Xu and A. Pich, *Polym. Chem.*, 2016, **7**, 5011-5022.
52. S. Harrisson, X. Liu, J.-N. Ollagnier, O. Coutelier, J.-D. Marty and M. Destarac, *Polymers*, 2014, **6**, 1437-1488.
53. M. Amann and O. Minge, in *Synthetic Biodegradable Polymers*, eds. B. Rieger, A. Künkel, G. W. Coates, R. Reichardt, E. Dinjus and T. A. Zevaco, Springer Berlin Heidelberg, 2012, vol. 245, pp. 137-172.
54. L. Etchenausia, A. M. Rodrigues, S. Harrisson, E. Deniau Lejeune and M. Save, *Macromolecules*, 2016, **49**, 6799-6809.
55. J. Liu, C. Detrembleur, M.-C. De Pauw-Gillet, S. Mornet, E. Duguet and C. Jérôme, *Polym. Chem.*, 2014, **5**, 799-813.
56. J. L. Pons, T. E. Malliavin and M. A. Delsuc, *Journal of biomolecular NMR*, 1996, **8**, 445-452.
57. J. Ramos, Á. Costoyas and J. Forcada, *J. Polym. Sci., Part A: Polym. Chem.*, 2006, **44**, 4461-4478.
58. C. S. Johnson, *Prog. Nucl. Magn. Reson. Spectrosc.*, 1999, **34**, 203-256.
59. BASF, *Safety Data Sheet*, 2012.
60. A. Imaz and J. Forcada, *Macromolecular Symposia*, 2009, **281**, 85-88.
61. G. Aguirre, J. Ramos and J. Forcada, *Soft Matter*, 2013, **9**, 261-270.
62. F. Schneider, A. Balaceanu, A. Feoktystov, V. Pipich, Y. Wu, J. Allgaier, W. Pyckhout-Hintzen, A. Pich and G. J. Schneider, *Langmuir*, 2014, **30**, 15317-15326.

63. M. J. Derry, L. A. Fielding, N. J. Warren, C. J. Mable, A. J. Smith, O. O. Mykhaylyk and S. P. Armes, *Chemical Science*, 2016, **7**, 5078-5090.
64. A. Sionkowska, *Prog. Polym. Sci.*, 2011, **36**, 1254-1276.
65. V. Delplace and J. Nicolas, *Nat Chem*, 2015, **7**, 771-784.